

Green Synthesis of Silver Nanoparticles as Saturable Absorber for Q-switched Fiber Laser

Nur Aina Aqilah Mohd Abd Jalil¹, Noor Ummi Hazirah Hani Zalkepli^{1*}

¹ Department of Physics and Chemistry, Universiti Tun Hussein Onn Malaysia, Kampus Cawangan Pagoh, Hab Pendidikan Tinggi Pagoh, KM 1, Jalan Panchor, 84600 Pagoh, Muar, Johor, MALAYSIA

*Corresponding Author: noorummi@uthm.edu.my
DOI: <https://doi.org/10.30880/ekst.2024.04.01.030>

Article Info

Received: 15 January 2024
Accepted: 16 January 2024
Available online: 27 July 2024

Keywords

Green synthesis, Silver nanoparticles, Q-switched, Saturable absorbers

Abstract

This study successfully demonstrated the generation of Q-switched fiber laser by using silver nanoparticles (AgNPs) as saturable absorber (SA) utilizing green synthesis approach. The synthesis of AgNPs involved the combination of green tea extract and a silver nitrate (AgNO₃) solution. Subsequently, to create a thin film containing the AgNPs as an SA, the resulting mixture was blended with a polyvinyl-alcohol (PVA) solution. The modulation depth and saturation intensity of AgNPs were determined to be 24.37% and 0.15 MW/cm², respectively. By incorporating the AgNPs thin film into a single-ring cavity, we achieved a stable Q-switched fiber laser at a maximum pump power of 190.30 mW. The Q-switched fiber laser exhibited a maximum pulse repetition rate of 56.93 kHz, the shortest pulse width of 2.00 μs, a maximum pulse energy of 0.2 nJ, and a signal-to-noise ratio (SNR) of 61.67 dB. These findings suggest that the AgNPs synthesized through the green synthesis approach performed effectively as a SA in the C-band region.

1. Introduction

Q-switching, or "Quenching Switching," is an advanced technique used in laser technology to generate pulsed laser beams with a very high peak power. The fundamental purpose of Q-switching is to store energy in the laser medium for an extended period of time before releasing it in the form of a short, strong pulse. This approach is essential in applications that require precise control and manipulation of laser pulses, such as medical operations, material processing, and communication systems [1]. The typical Q-switched Nd:YAG laser pulses, for example, have durations of 3-7 nanoseconds [2]. Q-switching employs methods such as Acoustic-optic Q-switching and passive Q-switching to generate short, high-intensity pulses. In Acoustic-optic Q-switching, an acoustic-optic modulator (AOM) within the laser cavity modulates the laser beam's intensity by periodically changing the refractive index of a crystal through which the beam passes. Adjusting the AOM's parameters controls the laser energy buildup, and when the AOM is switched to high-transmission, a powerful pulse is emitted [3] [4]. On the other hand, passive Q-switching involves incorporating saturable absorbers, like carbon nanotubes or graphene, into the laser cavity [5]. Initially, these absorbers saturate, absorbing laser light, but as intensity increases, they quickly become transparent, releasing a high-energy pulse when the laser gain surpasses cavity losses [6]. These Q-switching techniques find applications in various lasers, serving diverse purposes such as material processing and medical procedures by delivering intense, controlled laser pulses [7]. The choice between these techniques depends on the specific laser system, pulse characteristics, and application requirements. The material used for the generation of Q-switching typically involves biocompatible and environmentally friendly substances. Plant extracts, such as those derived from medicinal plants or algae, are commonly employed due to their ability to act

as reducing agents. These extracts contain bioactive compounds, such as polyphenols, flavonoids, and other organic molecules, which facilitate the reduction of silver ions to form AgNPs [8]. The characteristics of the resulting material include excellent biocompatibility, low toxicity, and eco-friendliness, making it suitable for various applications in biophotonics and biomedical fields [9]. The unique optical properties of AgNPs, such as their surface plasmon resonance, make them effective SA for Q-switched fiber lasers.

To initiate the green synthesis of AgNPs as a SA for Q-switched fiber lasers, start by preparing a green tea extract that serves as both a reducing and stabilizing agent. Boil green tea leaves in water to extract bioactive components such as catechins. In the meantime, make a silver nitrate solution as a precursor for AgNPs. Add the silver nitrate solution into the green tea extract to cause a reaction in which the bioactive components act as reducing agents, transforming silver ions into AgNPs. This reduction step produces well-stabilized nanoparticles with the advantages of green tea. To characterize the size, shape, and optical properties of the produced AgNPs, employ techniques such as UV-Vis spectroscopy, transmission electron microscopy (TEM) and scanning electron microscopy (SEM). Once characterized, integrate the green-synthesized AgNPs into the cavity of a Q-switched fiber laser, leveraging their unique properties for efficient pulse generation in laser applications. This integration acts as a saturable absorber, allowing the laser pulse to be tuned. A various range of AgNPs sizes may be produced by green synthesis techniques, making it difficult to achieve consistent characteristics. AgNPs' effectiveness as a SA may be affected by size variations [10]. The purity of green-synthesized AgNPs matters as contaminants in the synthesis process can affect their optical characteristics and effectiveness as a SA [11]. Fine-tuning synthesis parameters, such as the concentration of green tea extract, AgNO_3 , and reaction time, presents challenges. Optimization is necessary to achieve the desired AgNPs characteristics [12]. The green synthesis of AgNPs using green tea leaves as a reducing and stabilizing agent presents an environmentally sustainable and biocompatible approach for the preparation of SA in the context of Q-switched Fiber Lasers [13]. This process involves boiling green tea leaves, which are high in bioactive chemicals, to extract the essential components. The obtained green tea extract is then mixed with a AgNO_3 solution to initiate a reduction reaction in which the bioactive components act as natural reducing agents, allowing silver ions to be reduced to AgNPs. The benefits of this green synthesis method are significant, aligning with the principles of green chemistry by minimizing the use of hazardous chemicals and reducing environmental impact. This eco-friendly approach contributes to sustainable nanotechnology. Additionally, the availability of green tea as a source material makes this synthesis method cost-effective and sustainable, enhancing its scalability [14]. Numerous studies have explored biological techniques for AgNPs production, investigating sources such as fungi, bacteria, and algae, in addition to plants [15]. Because of its unique chemical constituents, green tea is frequently used to synthesize AgNPs as a saturable absorber for Q-switched fiber lasers. Green tea contains polyphenols, particularly catechins, which act as reducing agents, allowing the reduction of silver ions and the formation of AgNPs [16]. Furthermore, the antioxidant properties of green tea help to stabilize the formed nanoparticles [17][18]. This stability is necessary for their successful integration into Q-switched fiber lasers, where the SA plays an important role in pulse generation. Green tea-derived AgNPs are also biocompatible, which makes them suitable for a variety of applications, including biomedical and sensing devices.

Various types of green synthesis method have been reported to synthesize nanoparticles. *Eugenia jambolana* leaf extract was employed to synthesize AgNPs [19]. The synthesized AgNPs using aloe vera showed that AgNPs had a high antibacterial which depended on their synthesis conditions [20]. The synthesized of AgNPs by *Boerhaavia diffusa* plant extract reveals that AgNPs are in spherical shape with an average size of 24 nm [21].

Hence, this study utilizes green synthesis approach to fabricate AgNPs thin film as SA for generation of Q-switched fiber laser. The Q-switched fiber laser able to achieve maximum repetition rate of 56.93 kHz, pulse width of 2.00 μs , pulse energy of 0.20 nJ, average output power of 5.00 mW, and SNR of 61.67 dB.

2. Materials and Methods

2.1 Preparation of AgNPs as SA

Fresh young green tea leaves were harvested from Cameron Highlands, providing an alternative source for the green synthesis of AgNPs. Fig. 1 (a) shows the preparation of green tea extract where 20 g of fresh green tea leaves were washed by using deionized water to eliminate any dust and particles. Then, the leaves were cut and ground with a mortar and pestle to form a tea paste. The tea paste was then mixed with 50 mL of deionized water in a 100 mL round-bottom flask and stirred at room temperature for two hours. Subsequently, the mixture was left undisturbed for 30 minutes before filtering using Whatman filter paper to obtain green tea extract. Fig. 1 (b) shows the synthesis of AgNPs thin film as SA. This involved mixing 10 mL of silver nitrate solution with 100 mL of green tea extract, resulting in a change in the mixture's color to maroon, indicating the presence of the AgNPs. To create the AgNPs thin film, a mixture of 125 mL of PVA solution and 100 mL of the AgNPs solution was prepared and poured into a petri dish. The drying process was carried out in an oven at a temperature of 60°C for a duration of 6 hours.

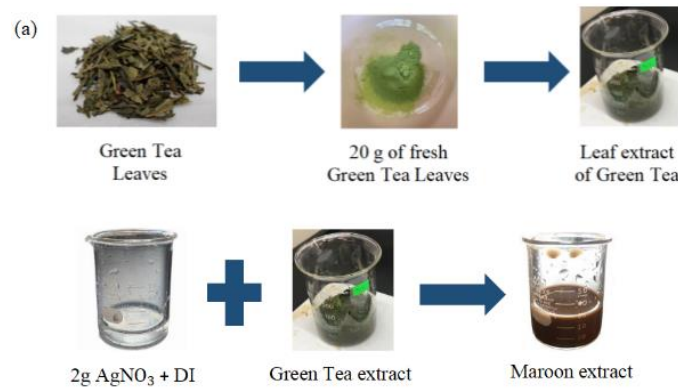


Fig. 1 a) Preparation of green tea leaf extract; b) Synthesis of AgNPs solution

2.2 Characterization of AgNPs as SA

Fig. 2 (a) illustrated the experimental setup of a twin-detector system designed for measuring the nonlinear absorption of AgNPs as a saturable absorber (SA). The experimental configuration included a homemade femtosecond laser with a repetition rate of 56 MHz, a pulse duration of 430 fs and operating wavelength of 1560 nm. An attenuator was positioned after the femtosecond laser source to regulate the output power and was then linked to a 50:50 optical coupler for splitting the light signal. Following the split, one port of the 50% optical coupler was connected to power meter 1, serving as a reference to read the power value. Simultaneously, the other port was connected to a fiber ferrule containing the AgNPs thin film. This fiber ferrule was then linked to power meter 2 to measure the output power. Fig. 2 (b) show the graph of nonlinear absorption, which fitted by using an equation below [22]:

$$\alpha(I) = \frac{\alpha_s}{1 + I/I_{sat}} + \alpha_{ns}$$

where α is absorption α_{ns} , is non-saturable loss, α_s is saturable absorption, I is intensity and I_{sat} is saturation intensity. Based on the figure, the modulation depth, non-saturable absorption, and saturation intensity of AgNPs thin film is 24.37 %, 4.92 % and 0.15 MW/cm².

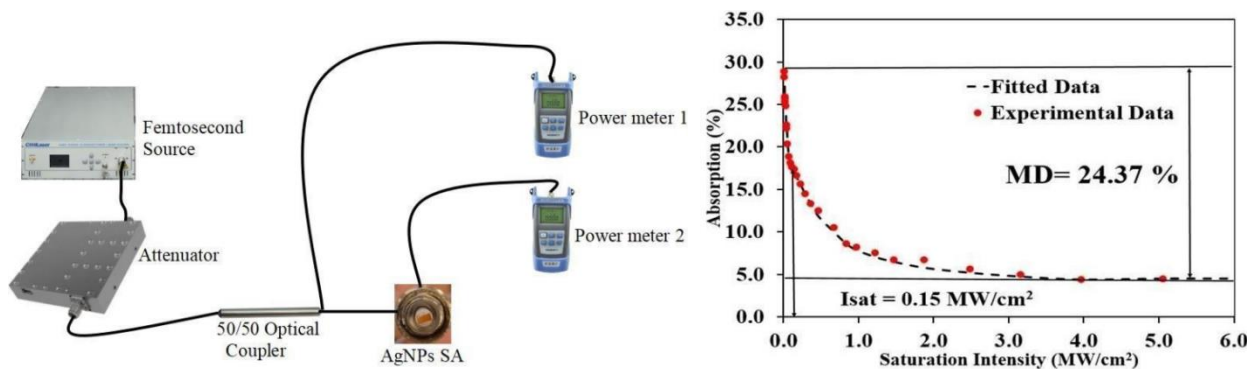


Fig. 2 (a) Twin detector system for measuring nonlinear absorption of AgNPs. (b) The graph of nonlinear absorption

In addition, the AgNPs was characterized by using scanning electron microscope (SEM) to observe the surface morphology and size of AgNPs. Fig. 3 (a) shows the surface morphology of AgNPs which exhibit a round shape of particles at magnification of x5.0 kV. To measure the absorption of AgNPs, UV-Vis was utilized at wavelength from 250 nm until 550 nm. The obvious absorption peak was observed at wavelength of 445 nm with absorbance of approximately 2.0 a.u. as depicted in Fig. 3 (b). The absorption spectra obtained through UV-Vis spectroscopy accurately confirmed the presence of AgNPs, as these nanoparticles displayed a pronounced absorption peak due to surface plasmon excitation in the UV range. Typically, AgNPs exhibit an absorption band around 420 nm. Smaller AgNPs tend to shift this band to approximately 420 to 430 nm, while larger AgNPs cause the band to

extend to around 430 nm to 445 nm. The observed widening of the peak suggested a wide dispersion of the particles. It is noteworthy that the size of nanoparticles is a crucial factor influencing photon excitation and the formation of absorption bands [fuhb]. Fig. 3 (c) shows the Fourier Transform Infrared Spectroscopy (FTIR) spectrum to determine molecular structure and chemical bonding of AgNPs. The FTIR spectrum of AgNPs was recorded within the wavenumber range of 600.10 to 3984.52 cm^{-1} . The complexity of the biological material is evident in the multiple peaks observed in the FTIR spectrum, including distinct peaks at 3213, 2915, 1629, 1040, and 820 cm^{-1} . The prominent peak at 3213 cm^{-1} corresponds to the broad absorption of the -OH group, characteristic of polyols like hydroxyflavones and catechins.

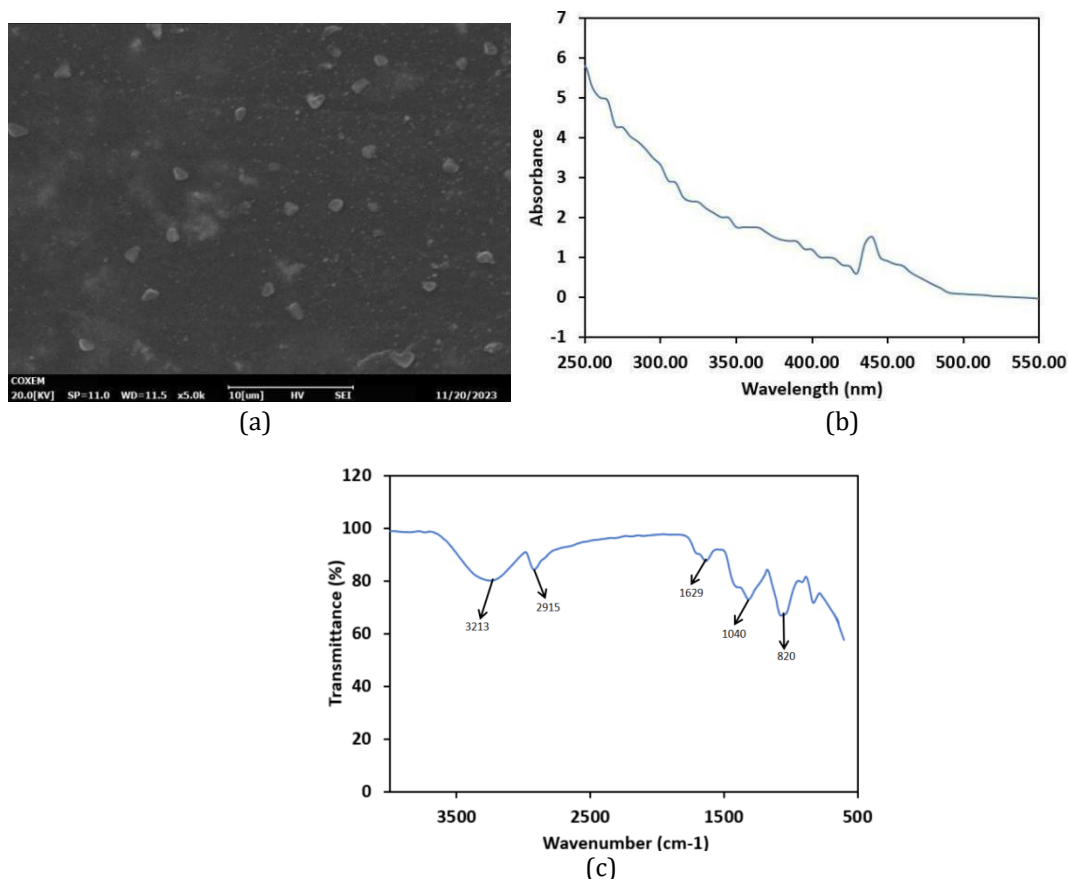


Fig. 3 (a) Surface morphology of AgNPs using SEM; (b) The absorption of AgNPs using UV-Vis spectroscopy; (c) FTIR spectrum of AgNPs.

2.3 Experimental design of Q-switched

Fig. 4 illustrates the setup of the Q-switched fiber laser incorporating AgNPs thin film as SA. A 3.00 m length erbium-doped fiber (EDF), a 980/1550 nm wavelength division multiplexer (WDM), an optical isolator, a 10/90 output coupler (OC) and a 980 nm laser diode (LD) were used to construct a single ring cavity. The EDF as gain media was pumped using LD through the WDM. The end of the EDF was spliced with ISO isolator to guarantee that light traveled only in single direction. The AgNPs thin film was sandwiched between two fiber ferrules to act as SA and integrated inside the cavity after the isolator. To complete the single ring cavity, the 90:10 OC was linked after the SA, where 90 % port of OC was spliced with 1550 nm port of WDM. Meanwhile, the 10% port of OC was connected to 50:50 OC. Both port of 50% was joined for monitoring the optical spectrum using an optical spectrum analyzer (OSA) and observing the time and frequency domain of the Q-switched system using an oscilloscope (OSC).

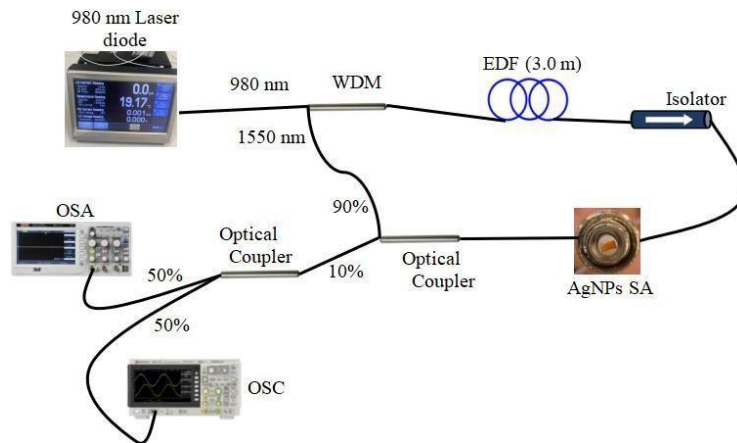


Fig. 4 Q-switched fiber laser using AgNPs schematic diagram

3. Results and Discussion

A stable Q-switched fiber laser was observed after inserting the SA and increased the pump laser. At pump power of 33.10mW, the pulse optical spectrum of the Q-switched depicts in Fig 5 (a). The laser is operated at 1569.00 nm central wavelength at 1.0 nm resolution. The 3-dB bandwidth is 0.60 nm. Fig 5 (b) displays the pulse optical spectrum of the Q-switched at a pump power of 190.30 mW with a 1.0 nm resolution, the central wavelength of 1568.20 nm was detected. The broader bandwidth is 4.60 nm, which broadens caused by self-phase modulation (SPM) effect [23].

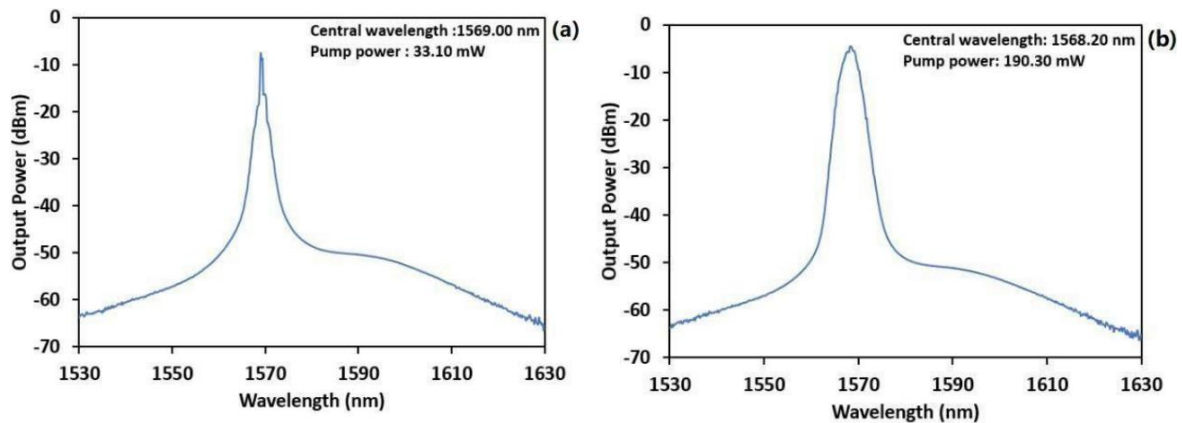


Fig. 5 (a) The laser performance at 33.10mW pump power; (b) The laser performance at 190.30 mW pump power.

Fig 6 (a) shows the pulse train when the pump power is set to a minimum of 33.10 mW. the short pulse width is 8.80 μ s with time difference between the two pulses is 43.30 μ s. The peak amplitude remains relatively constant at around 0.01 V, indicating a consistent pulse train. However, the pulse train does not show any significant amplitude fluctuations; instead, it appears to maintain a consistent pulse shape and intensity. The typical pulse train is displayed in Fig 6 (b) at the highest pump power of 190.30 mW with the short pulse width of 4.10 μ s. The 17.60 μ s time difference between the two pulses. At about 0.018 V, the peak amplitude stays comparatively constant, suggesting a steady pulse train. The Q-switched stability can be seen by its consistent pulse shape, intensity, and amplitude across various pump powers. The ability to maintain a consistent pulse rate is a positive performance characteristic. The change in time difference between pulses with varying pump powers indicates control over the pulse repetition rate. This modulation is unique to Q-switched lasers and allows for more flexibility in pulse generation. The Q-switched laser system's ability to maintain a relatively constant peak amplitude across different pump powers reflects its stable performance.

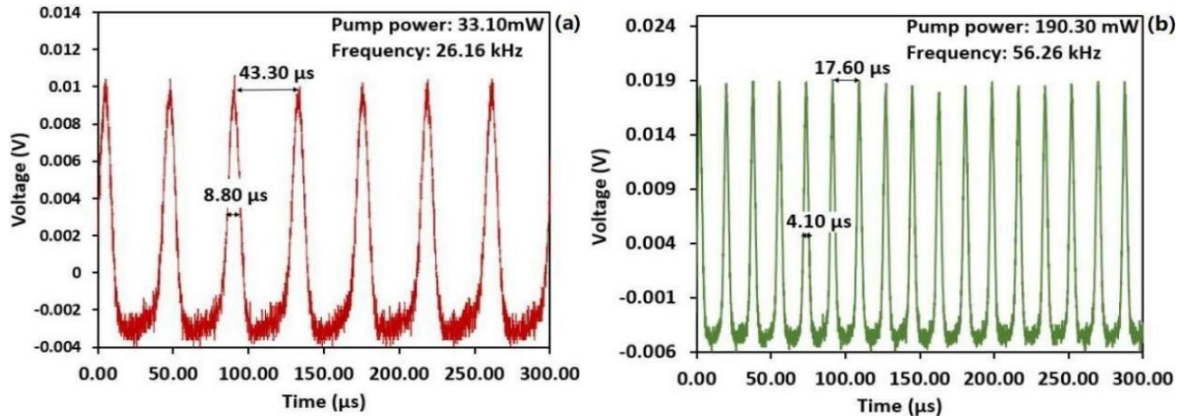


Fig. 6 (a) Typical pulse train at 33.10 mW pump power; (b) pulse train at 190.30 mW pump power

Fig 7 (a) demonstrates the fundamental frequency of 26.16 kHz at pump power of 33.10 mW. Furthermore, the signal-to-noise ratio (SNR) is 54.00 dB, with a resolution bandwidth (RBW) of 300 Hz and span of 300 kHz of with nine harmonics. At maximum pump power of 190.30 mW, the fundamental frequency is of 56.26 kHz was demonstrated with SNR of 61.67 dB as shown in Fig 7 (b). This indicates that the pulses that were produced were highly stable and matched those from other similar operations [24,25].

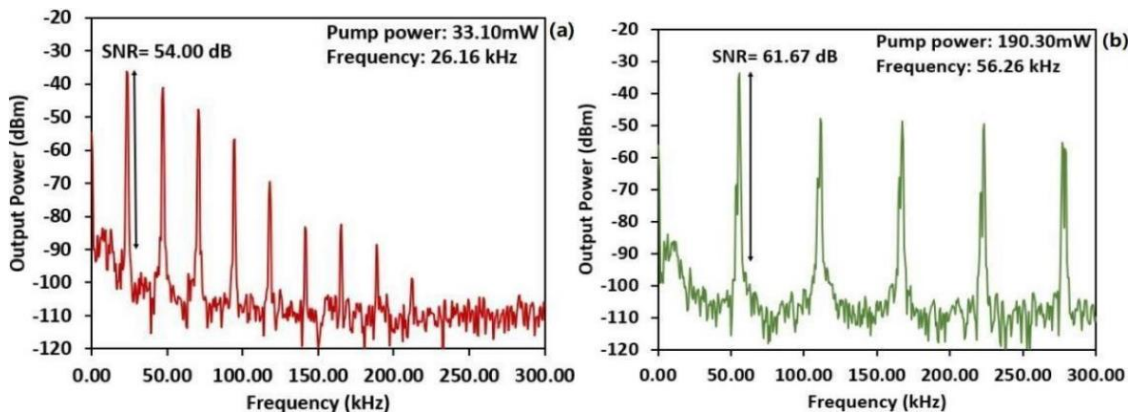


Fig. 7 (a) RF spectrum at the minimum pump power of 33.10 mW; (b) RF spectrum at the maximum pump power of 190.30 mW

The examination of both the repetition rate and pulse width of a Q-switched was investigated by changing the pump power from 33.10 mW to 190.30 mW. Fig. 8 shows the pulse width narrows swiftly from 4.9 μs to 2.0 μs as the pump power increases from 33.10 mW to 190.10 mW. On the other hand, the repetition rate steadily rises from 23.16 kHz to 56.93 kHz at pump power of 33.10 mW to 190 mW.

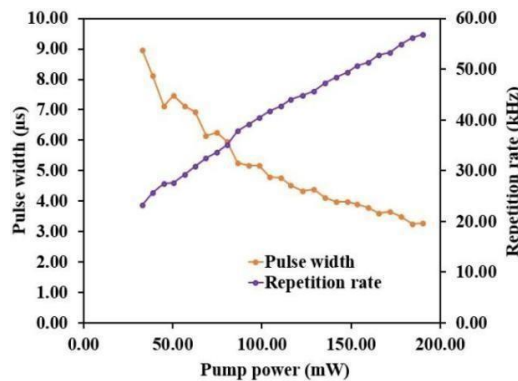


Fig. 8 The pulse width and repetition rate versus tuned wavelength at pump power of 190.30 mW

Fig 9 shows the patterns in the of average output power and pulse energy against pump power. The average output power and pulse energy increased as the pump power increased from 0.05 nJ to 0.20 nJ and 1.20mW to 5.00mW, respectively.

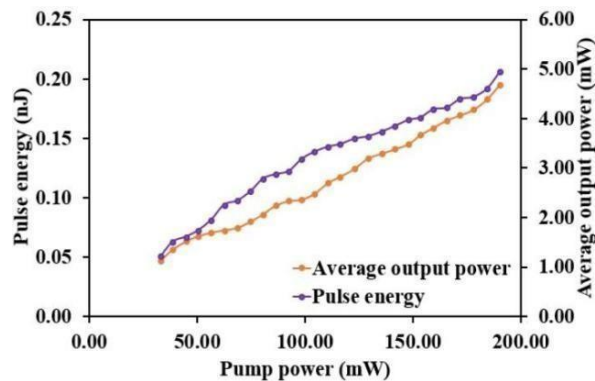


Fig. 9 The average output power and pulse energy versus pump power

4. Conclusion

In conclusion, we successfully demonstrated the generation of a Q-switched fiber laser using AgNPs as a SA through a green synthesis approach. The AgNPs were synthesized by combining green tea extract with a silver nitrate (AgNO₃) solution, and the resulting mixture was blended with a polyvinyl-alcohol (PVA) solution to form a thin film. The AgNPs exhibited a modulation depth of 24.37% and a saturation intensity of 0.15 MW/cm². Incorporating the AgNPs thin film into a single-ring cavity resulted in a stable Q-switched fiber laser with notable parameters, including a maximum pump power of 190.30 mW, a maximum pulse repetition rate of 56.93 kHz, the shortest pulse width of 2.00 μs, a maximum pulse energy of 0.2 nJ, and a SNR of 61.67 dB. These findings underscore the effective performance of AgNPs synthesized through green synthesis as a SA in the C-band region for generation of pulse fiber laser which can be applied in optical communication system.

Acknowledgement

The authors would like to express their sincere gratitude to the Government of Malaysia and Universiti Tun Hussein Onn Malaysia for their support in funding this research project.

Conflict of Interest

There is no conflict of interest in the publication of the paper.

Author Contribution

The authors confirm contribution to the paper as follows: **study conception and design, data collection, methodology, analysis and interpretation of results:** Nur Aina Aqilah Mohd Abd Jalil and Noor Umami Hazirah Hani Zalkepali. All authors reviewed the results and approved the final version of the manuscript.

References

- [1] Bawden, N., Matsukuma, H., Henderson-Sapir, O., Klantsataya, E., Tokita, S., & Ottaway, D. J. (2018, February). Q-switched dual-wavelength pumped 3.5-μm erbium-doped mid-infrared fiber laser. In *Fiber Lasers XV: Technology and Systems* (Vol. 10512, pp. 121-126). SPIE.
- [2] Goel, A. (2008). Clinical applications of Q-switched NdYAG laser. *Indian journal of dermatology, venereology and leprology*, 74, 682.
- [3] Harb, C. C. (1992). Stabilization of a ring dye laser.
- [4] Posts, V. M. (2020, August 10). Q-switches: Passive vs Active? The Laser-IPL Guys. <https://thelaseriguysblog.wordpress.com/2020/08/10/q-switches-passive-vs-active/>
- [5] Ismail, M. A., Harun, S. W., Ahmad, H., & Paul, M. C. (2016). Passive Q-switched and mode-locked fiber lasers using carbon-based saturable absorbers. *Fiber Laser*, 43-69.
- [6] Kivistö, S. (2010). Short pulse lasers using advanced fiber technology and saturable absorbers.
- [7] El-Sherif, A. F. (2003). Pulsed optical fibre lasers: Self-pulsation, Q-switching and tissue interactions. The University of Manchester (United Kingdom).

- [8] Huq, M. A., Ashrafudoulla, M., Rahman, M. M., Balusamy, S. R., & Akter, S. (2022). Green synthesis and potential antibacterial applications of bioactive silver nanoparticles: A review. *Polymers*, 14(4), 742.
- [9] ZAHKAN, H. (2022). BIOACTIVITY CHARACTERISTICS OF SILVER NANOPARTICLES SYNTHESIZED BY STREPTOMYCES SP. BSP1 (Doctoral dissertation, Ondokuz Mayıs University).
- [10] Karade, V. C., Patil, R. B., Parit, S. B., Kim, J. H., Chougale, A. D., & Dawkar, V. V. (2021). Insights into shape-based silver nanoparticles: a weapon to cope with pathogenic attacks. *ACS Sustainable Chemistry & Engineering*, 9(37), 12476-12507.
- [11] Awang, N. A., Zulkefli, N. U. H. H., Zamri, A. Z. M., Mahmud, N. N. H. E. B. N., & Muhammad, N. A. M. Enhanced Tunability of Q-Switched Fiber Lasers Using Biogenic Agnps-Cs Saturable Absorber: Optical Deposition vs. Drop Casting. *NAM, Enhanced Tunability of Q-Switched Fiber Lasers Using Biogenic Agnps-Cs Saturable Absorber: Optical Deposition vs. Drop Casting*.
- [12] Silva, L., Pereira, T. M., & Bonatto, C. C. (2019, January 1). *Frontiers and perspectives in the green synthesis of silver nanoparticles*. Elsevier eBooks. <https://doi.org/10.1016/b978-0-08-102579-6.00007-1>
- [13] Shanker, U., Jassal, V., Rani, M., & Kaith, B. S. (2016). Towards green synthesis of nanoparticles: from bio-assisted sources to benign solvents. A review. *International Journal of Environmental Analytical Chemistry*, 96(9), 801-835
- [14] Fu, H. B., & Yao, J. N. (2001). Size effects on the optical properties of organic nanoparticles. *Journal of the American Chemical Society*, 123(7), 1434-1439.
- [15] Rónavári, A., Igaz, N., Adamecz, D. I., Szerencsés, B., Molnar, C., Kónya, Z., ... & Kiricsi, M. (2021). Green silver and gold nanoparticles: Biological synthesis approaches and potentials for biomedical applications. *Molecules*, 26(4), 844.
- [16] Kharabi Masooleh, A., Ahmadikeh, A., & Saidi, A. (2019). Green synthesis of stable silver nanoparticles by the main reduction component of green tea (*Camellia sinensis* L.). *IET nanobiotechnology*, 13(2), 183-188.
- [17] Flieger, J., Franus, W., Panek, R., Szymańska-Chargot, M., Flieger, W., Flieger, M., & Kołodziej, P. (2021). Green synthesis of silver nanoparticles using natural extracts with proven antioxidant activity. *Molecules*, 26(16), 4986.
- [18] Aryani, R., Hidayat, A. F., Darma, G. C. E., & Utami, O. (2019, November). Effect of solid lipid nanoparticles system on the stability of Green Tea leaves (*Camellia sinensis* L. Kuntze) extract as sunscreen. In *Journal of Physics: Conference Series* (Vol. 1375, No. 1, p. 012078). IOP Publishing.
- [19] Gomathi, S., Firdous, J., & Bharathi, V. (2017). Phytochemical screening of silver nanoparticles extract of *Eugenia jambolana* using Fourier infrared spectroscopy. *Int J Res Pharm Sci*, 8(3), 383-387.
- [20] Tippayawat, P., Phromviyo, N., Boueroy, P., & Chompoosor, A. (2016, October 19). Green synthesis of silver nanoparticles in aloe vera plant extract prepared by a hydrothermal method and their synergistic antibacterial activity. *PeerJ*, 4, e2589. <https://doi.org/10.7717/peerj.2589>
- [21] Kumar, P. V., Pammi, S. V. N., Kollu, P., Satyanarayana, K. V. V., & Shameem, U. (2014). Green synthesis and characterization of silver nanoparticles using *Boerhaavia diffusa* plant extract and their anti bacterial activity. *Industrial Crops and Products*, 52, 562-566.
- [22] Zalkepli, N. U. H. H., Awang, N. A., Ghosh, B. K., Mohamad, K. A., Alias, A., Mahmud, N. N. H. E. N., ... & Muhammad, N. A. M. (2023). Tunable performance of indium tin oxide-zinc oxide as Q-switcher. *Optik*, 281, 170852.
- [23] Renninger, W. H., Chong, A., & Wise, F. W. (2010). Self-similar pulse evolution in an all-normal-dispersion laser. *Physical Review A*, 82(2), 021805.
- [24] SATRIA, A. H. B. M. (2022). Isolation and characterization of biosurfactant-producing lactic acid bacteria from sauerkraut. *Enhanced Knowledge in Sciences and Technology*, 2(2), 060-069.
- [25] Muhammad, N. A. M., Awang, N. A., Mahmud, N. N. H. E. N., Zalkepli, N. U. H. H., Zamri, A. Z. M., Basri, H., & Rasli, N. I. (2023). Biosynthesized zinc oxide and titanium dioxide nanoparticles by aloe vera extract for tunable Q-switched application. *Optical Fiber Technology*, 77, 103276.